

## Interaction of dislocations with carbides in BCC Fe studied by molecular dynamics

F. Granberg,<sup>1, a)</sup> D. Terentyev,<sup>2</sup> K. O. E. Henriksson,<sup>1</sup> F. Djurabekova,<sup>3</sup> and K. Nordlund<sup>1</sup>

<sup>1)</sup>*Department of Physics, P.O. Box 43, FIN-00014 University of Helsinki, Finland*

<sup>2)</sup>*Nuclear Materials Science Institute, SCK-CEN, Boeretang 200 B-2400, Mol, Belgium*

<sup>3)</sup>*Helsinki Institute of Physics and Department of Physics, P.O. Box 43, FIN-00014 University of Helsinki, Finland*

(Dated: 23 October 2013)

Iron carbide ( $\text{Fe}_3\text{C}$ ), also known as cementite, is present in many steels, and may due to radiation be destroyed into nanosized precipitates. We examine the interaction of edge dislocations with nanosized cementite precipitates in Fe by molecular dynamics. The simulations are carried out with a Tersoff-like bond order interatomic potential by Henriksson *et al.* for Fe-C-Cr systems. Comparing the results obtained with this potential for a defect free Fe system with results from previously used potentials, we find that the potential by Henriksson *et al.* gives significantly higher values for the critical stress, at least at low temperatures. The results show that edge dislocations can penetrate cementite precipitates of sizes 1 nm and 2 nm even at a temperature of 1 K, although the stresses needed for this are high. On the other hand, a 4 nm precipitate is impenetrable for edge dislocations at low temperatures ( $\leq 100$  K) on our simulation timescale.

Keywords: dislocation, molecular dynamics, cementite, precipitate

---

<sup>a)</sup>Electronic mail: fredric.granberg@helsinki.fi

## I. INTRODUCTION

Steel in its many various forms represents the main structural material of both current fission and future fusion power plants. To safely build new nuclear power plants or to run the old ones even longer, research in reactor materials and in particular steels must be carried out. Many steels contain iron carbide ( $\text{Fe}_3\text{C}$ ), also known as cementite. The cementite in steels can possibly be destroyed into nanosized precipitates, due to the high levels of radiation present. How these nanosized precipitates will affect the mechanical properties of steel is not yet known. To start investigating this phenomenon, we used atom-level classical molecular dynamics (MD) simulations. The newly developed interatomic potentials, Henriksson *et al.*<sup>1</sup> and Hepburn and Ackland<sup>2</sup>, have made it possible to simulate systems with both Fe and C. In this investigation we use the Henriksson *et al.* potential<sup>1</sup> and compare results for a single edge dislocation in defect free Fe with other studies<sup>3,4</sup>. The interaction between an edge dislocation and nanosized cementite precipitates is also investigated. In this study we focus on the effects of the size of the precipitates and the temperature of the system.

## II. METHODS

In this investigation we used the classical molecular dynamics code PARCAS<sup>5,6</sup> and a dislocation simulation method suggested by Osetsky and Bacon<sup>7</sup>. We used an interatomic potential by Henriksson *et al.* (H13)<sup>1</sup>, a Tersoff-like bond order potential (BOP). Our simulation cell consisted of a block of Fe in BCC structure with the axes oriented along  $[\bar{1}\bar{1}2]$ ,  $[111]$  and  $[1\bar{1}0]$  directions and a single edge dislocation placed in the center of the cell. The Burger's vector of the edge dislocation was  $1/2 a_{111} [111]$ , where  $a_{111}$  is the lattice constant in  $[111]$  direction. Following the procedure presented in Ref. 7, the few lowermost and uppermost layers of atoms were fixed and a Berendsen type thermostat<sup>8</sup> was applied to a few layers of atoms over the fixed atoms at the bottom. Periodic boundary conditions (PBC) were applied in the two non fixed directions. A schematic figure of the simulation cell is presented in Fig. 1. To visualize the dislocation movement and to get qualitative results the program OVITO and an adaptive common neighbour analysis by Stukowski was used.<sup>9</sup>

In the investigation of a single edge dislocation in defect free iron, a simulation cell of 325000 atoms – of which 265000 were mobile – was used. The box size was  $21.2 \times 14.9 \times$

12.3 nm<sup>3</sup>, where the dislocation length is 21.2 nm, but over the PBC it can be considered infinitely long. This size will result in a dislocation velocity of 6.2 m/s according to the Orowan relation<sup>10</sup> with a strain rate of 10<sup>7</sup> 1/s. The Orowan relation describes how the strain rate,  $\gamma$ , is affected by the Burger's vector,  $b$ , dislocation density,  $\rho$ , and dislocation velocity,  $v$ , according to this equation:  $\gamma = b\rho v$ . From this equation the dislocation velocity can be determined for a given strain rate. Experimental values obtained for the edge dislocation velocity are between 10<sup>-4</sup> to 10<sup>-2</sup> m/s.<sup>11</sup> To determine the critical stress in defect free iron we used different constant strain rates, 10<sup>8</sup>, 5 × 10<sup>7</sup>, 10<sup>7</sup> and 5 × 10<sup>6</sup> 1/s. The strain was applied by displacing the fixed atoms at the upper region in the [111] direction, whereas the lower fixed atoms were not moved. The shear stress induced can be calculated from the formula  $\tau = F_y/A_{yx}$ , where  $F_y$  is the force on the upper fixed block in y-direction and  $A_{yx}$  is the area of the box in the yx-plane. The strain was applied after a relaxation period of  $\sim 10$  ps at the desired temperature. The temperatures used were 1 K, 10 K, 50 K and 100 K.

In the simulations with a cementite precipitate a box with double the length between dislocations, in the same direction as the dislocation Burger's vector, was used. This results in a cell with 650000 atoms, of which 530000 were mobile. This was done to achieve a long enough distance between the precipitates over the PBC. The corresponding box size was 21.2 × 29.9 × 12.3 nm<sup>3</sup>. The length of the dislocation between the precipitates over PBC in these simulations was 21.2 nm -  $d_p$ , where  $d_p$  is the diameter of the precipitate. The Orowan relation for these systems gives a dislocation velocity of 12.3 m/s. To obtain the simulation cells for the cementite investigations, a void was cut out from the block with an edge dislocation. The cementite precipitate was cut out from a block of perfect Fe<sub>3</sub>C, space group Pnma (62)<sup>12</sup> of the same size as the void, shrunk by 5%<sup>13</sup> and placed inside the void. The lattice parameters for the Fe<sub>3</sub>C block were obtained according to the experimental values given in ref. 12 and references therein. The void and precipitate were placed so that the center of the void and precipitate were at the same level as the dislocation core and about 13 nm from the dislocation core. Three different sizes of the precipitates, 1 nm, 2 nm and 4 nm, containing 8, 116 and 876 carbon atoms, were used. The precipitate simulations lasted over 4 ns each, long enough for the dislocation to penetrate the precipitate at least a few times. The temperatures used for these simulations were 1 K, 10 K, 100 K and 500 K.

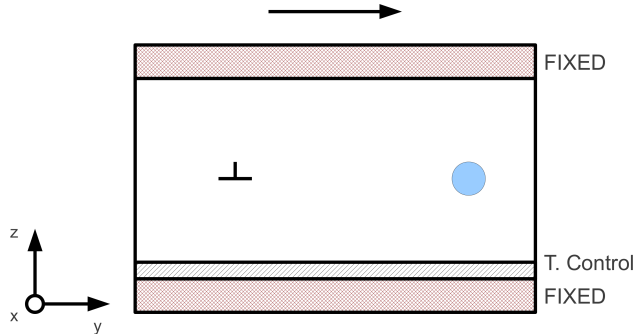


FIG. 1. Schematic illustration of the system setup

### III. RESULTS AND DISCUSSION

The results for a single edge dislocation in defect free Fe can be seen in Table I. In this table the critical stress and critical strain needed to initiate the dislocation movement is listed for a strain rate of  $10^7$  1/s. The results show that the critical stress is very high at low temperatures, but decreases significantly when the temperature rises. If these results are compared with previous results for similar systems, we see that the used potential will give substantially higher results at least at low temperatures. For instance the Ackland *et al.* potential from 2004 (A04)<sup>14</sup> gives the critical stress as  $\sim 90$  MPa and  $\sim 50$  MPa for 0 K and 1 K temperatures, respectively.<sup>3</sup> The difference seen at least at low temperatures should be attributed to the difference in the potential types, which apparently provide different core structures and stacking fault energy profiles. The A04 potential<sup>14</sup> is an Embedded Atom Model (EAM) potential but the H13 potential<sup>1</sup> is a Tersoff like BOP. The biggest difference is that the BOP has an angular dependence which the EAM potential does not. This can explain why it is hard to break the bonds and induce shear at low temperatures, needed to get the dislocation mobile. A detailed study of the dislocation structure and Peierls stress will follow.

In Fig. 2 the evolution of shear stress at different strain rates is compared at 10 K for simulations done in defect free crystals. From the figure it is clear that a lower strain rate will yield a lower critical stress, consistent with the thermally activated nature of dislocation slip. For the precipitate simulations we chose a strain rate of  $10^7$  1/s to achieve a compromise between accuracy and computational efficiency. This strain rate and faster ones have been used in earlier studies.<sup>3,4</sup> In our simulations we obtain the shear modulus for the potential to

be about 68 GPa for our specific system setup, which is close to the Ackland potentials<sup>14,15</sup> and Dudarev and Derlet potential<sup>16</sup>. The Ackland potentials give 65 GPa and 62 GPa<sup>3</sup> and the Dudarev and Derlet potential 75.6 GPa as the shear modulus.<sup>4</sup> The critical stress needed for an edge dislocation to penetrate cementite precipitates can be found in Table II. The critical stresses for the first penetration for different sizes of precipitates and temperatures are listed there. The values marked with a star are the cases where the edge dislocation could not penetrate the precipitate before it interacted with itself over the PBC. The value given in the table for these cases is the stress needed to generate a screw-dipole.

The results for the 1 nm, 2 nm and 4 nm cementite precipitates with the strain rate of  $10^7$  1/s are visualized in Fig. 3, Fig. 4 and Fig. 5, respectively. In the figure for 1 nm precipitates, Fig. 3, there is a clear point when the dislocations are unpinned from the precipitates. The difference between the peak heights and the stress between the peaks can, at least partially, be explained by jogs induced and vacancies created. The precipitate is at all temperatures split into two parts due to the dislocation movement and the hard shearing after the four or five penetrations. In the figure for 2 nm precipitates, Fig. 4, we also see differences in the heights due to the same phenomenon as for the 1 nm precipitate. In the 10 K case, one can see that something not self-evident happens after the second pass-through. The explanation for this behaviour is that the screw-dipole induced cannot close before the edge dislocation intersects with the precipitate a second time. The 2 nm precipitate stays together during the simulation, but is sheared due to the interactions with the edge dislocation, see Fig. 6. In this figure the precipitates are visualized before the shearing started and after the simulation and only the carbon atoms are visualized for clarity. From Fig. 5 we see that the edge dislocation cannot unpin from the 4 nm precipitate at low temperatures, before it hits the precipitate again. The dislocation can unpin from the 4 nm precipitate at 500 K. At the lower temperatures, the screw dipole does not have enough time to close or the sufficient thermal activation that is required to complete this event. This is why only the stress needed for creation of a screw-dipole is listed in Table II. This value can be used as a minimum for the stress needed to penetrate the corresponding precipitate.

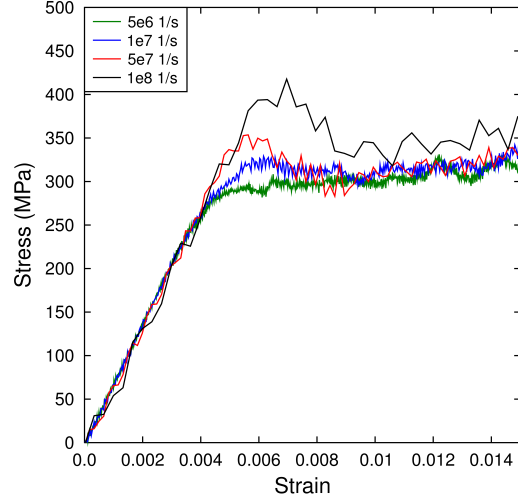


FIG. 2. Results from different strain rates at 10K for defect free Fe

Temperature	0 K	1 K	10 K	50 K	100 K
Critical Stress	745 MPa	494 MPa	328 MPa	~ 70 MPa	~ 30 MPa
Critical Strain	0.0108	0.0071	0.0063	~ 0.0011	~ 0.0006

TABLE I. Critical stress and strain for a single edge dislocation in defect free Fe at different temperatures

Diameter \ Temperature	Temperature			
	1 K	10 K	100 K	500 K
1 nm	1750 MPa	1750 MPa	380 MPa	140 MPa
2 nm	2450 MPa	2140 MPa	1080 MPa	290 MPa
4 nm	2260* MPa	2200* MPa	1100* MPa	550 MPa

TABLE II. Critical stresses for different sizes of the precipitates and different temperatures. The star indicates that in these cases the dislocation is not unpinned from the obstacle before it interacts with it again over the periodic boundaries; the value is the needed stress for creation of a screw-dipole (see text).

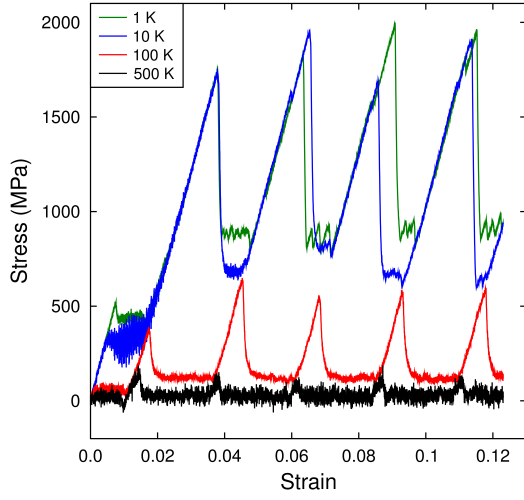


FIG. 3. Results for a 1 nm cementite precipitate

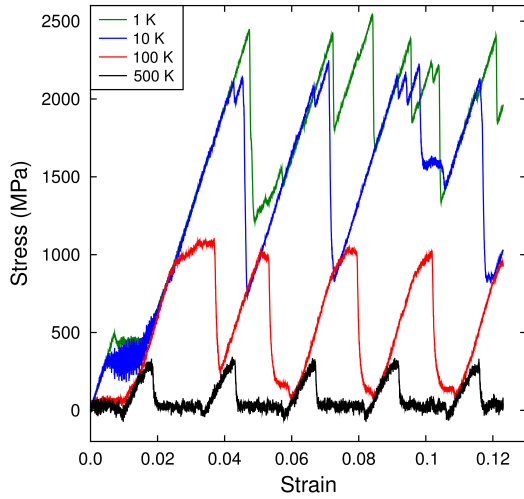


FIG. 4. Results for a 2 nm cementite precipitate

#### IV. CONCLUSIONS

In this investigation we have studied the behaviour of a single edge dislocation in BCC Fe using a bond order potential, when it interacts with nanoscale cementite precipitates of different sizes and at different temperatures. We have compared our results, obtained

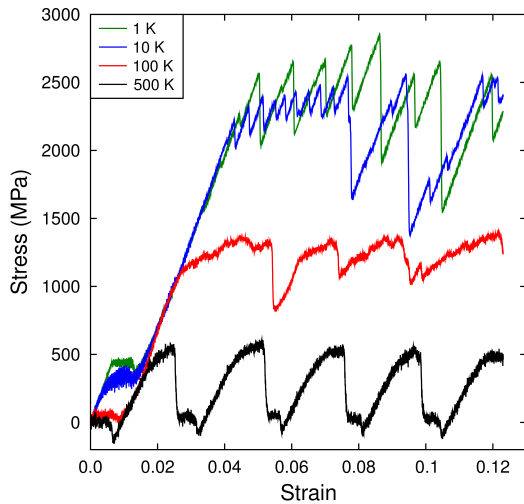


FIG. 5. Results for a 4 nm cementite precipitate

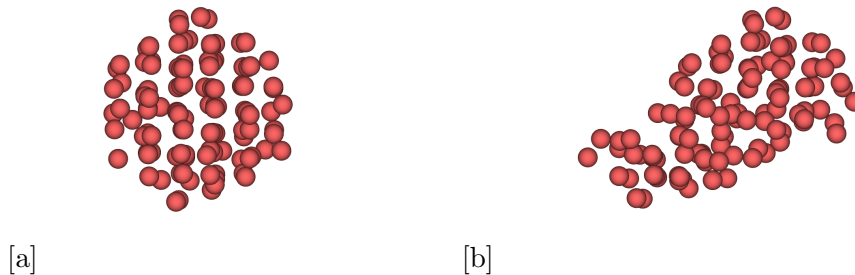


FIG. 6. A 2 nm precipitate before (a) the simulation and after (b) the simulation at 10 K. Only the carbon atoms are shown for clarity

using the H13 potential<sup>1</sup>, for a single edge dislocation in defect free Fe with results from other potentials. Our results show that the used potential gives significantly higher critical stresses to initiate dislocation movement at low temperatures. The results with cementite obstacles show that an edge dislocation can penetrate cementite precipitates of sizes 1 nm and 2 nm at temperatures as low as 1 K. The 4 nm precipitate is not sheared by the edge dislocation at low temperatures ( $\leq 100$  K).



## V. ACKNOWLEDGMENTS

This reaserch was funded by the Academy of Finland project SIRDAME (grant no. 259886). We thank the IT Center for Science CSC for granted computational resources.

## REFERENCES

- <sup>1</sup>K. O. E. Henriksson, C. Björkas, and K. Nordlund, *Journal of Physics: Condensed Matter* **25**, 445401 (2013).
- <sup>2</sup>D. J. Hepburn and G. J. Ackland, *Phys. Rev. B* **78**, 165115 (2008).
- <sup>3</sup>D. Terentyev, D. J. Bacon, and Y. N. Osetsky, *Journal of Physics: Condensed Matter* **20**, 445007 (2008).
- <sup>4</sup>S. M. Hafez Haghghat, J. Fikar, and R. Schäublin, *Journal of Nuclear Materials* **382**, 147 (2008).
- <sup>5</sup>K. Nordlund, M. Ghaly, R. S. Averback, M. Caturla, T. Diaz de la Rubia, and J. Tarus, *Phys. Rev. B* **57**, 7556 (1998).
- <sup>6</sup>M. Ghaly, K. Nordlund, and R. S. Averback, *Phil. Mag. A* **79**, 795 (1999).
- <sup>7</sup>Y. N. Osetsky and D. J. Bacon, *Modelling and Simulation in Materials Science and Engineering* **11**, 427 (2003).
- <sup>8</sup>H. J. C. Berendsen, J. P. M. Postma, W. F. van Gunsteren, A. DiNola, and J. R. Haak, *The Journal of Chemical Physics* **81**, 3684 (1984).
- <sup>9</sup>A. Stukowski, *Modelling and Simulation in Materials Science and Engineering* **18**, 015012 (2010).
- <sup>10</sup>V. V. Bulatov and W. Cai, *Computer simulations of dislocations*, Oxford series on materials modelling (Oxford University Press, Oxford, New York, 2006).
- <sup>11</sup>A. P. L. Turner and T. Vreeland Jr, *Acta Metallurgica* **18**, 1225 (1970).
- <sup>12</sup>W. C. C. Jr. and E. A. Carter, *Surface Science* **530**, 88 (2003).
- <sup>13</sup>F. Djurabekova and K. Nordlund, *Phys. Rev. B* **77**, 115325 (2008).
- <sup>14</sup>G. J. Ackland, M. I. Mendeleev, D. J. Srolovitz, S. Han, and A. V. Barashev, *Journal of Physics: Condensed Matter* **16**, S2629 (2004).
- <sup>15</sup>G. Ackland, D. Bacon, A. Calder, and T. Harry, *Philosophical Magazine A: Physics of Condensed Matter, Structure, Defects and Mechanical Properties* **75**, 713 (1997).

<sup>16</sup>S. Dudarev and P. Derlet, *Journal of Physics Condensed Matter* **17**, 7097 (2005).